PROCEEDINGS OF THE SOCIETY FOR EXPERIMENTAL BIOLOGY AND MEDICINE **180,** 62–71 (1985)

Arteriolar and Systemic Autoregulatory Responses during the Development of Hypertension in the Spontaneously Hypertensive Rat (42144)

ROY L. ALSON, JERRY W. DUSSEAU, AND PHILLIP M. HUTCHINS

Department of Physiology and Pharmacology, Bowman Gray School of Medicine, Wake Forest University, Winston-Salem, North Carolina 27103

Abstract. Pressure–flow curves were constructed to determine whether acute autoregulation in rat skeletal muscle was altered during the development of hypertension in the spontaneously hypertensive rat (SHR). Under chloralose:urethane anesthesia, hindlimb blood flow and pressure, plus diameter changes of gracilis muscle arterioles, were simultaneously measured in the 6- and 9-week Wistar–Kyoto (WKY) and SHR. Femoral blood flow was measured by electromagnetic flowmetry and hindlimb pressure controlled with an hydraulic occluder. Arteriolar diameters were measured using image shearing techniques. Acute autoregulatory capacity was assessed by comparing the closed-loop gain and the regression lines over the regulated and passive pressure ranges of the pressure–flow curves. The lower pressure limit of autoregulation (LPLAR) shifted upward as the blood pressure increased in the SHR with age; it did not shift in the WKY. Resting hindlimb flow, elevated in the SHR at 6 weeks, was also elevated at the LPLAR. At 9 weeks hindlimb blood flow was comparable in the WKY and SHR. As blood pressure was increased autoregulation was accompanied by vasoconstriction of gracilis arterioles. However, neither the gain of the autoregulatory system nor the regression lines describing the pressure–flow curves were different between the hypertensive and normotensive animals at either age. These results indicate that the acute autoregulatory response mechanism was not affected by the developing hypertension in the SHR, and is consistent with a structural basis for the chronic maintenance of the elevated peripheral vascular resistance.

In several models of hypertension the onset of the blood pressure increase is characterized by normal peripheral vascular resistance, but a higher than normal cardiac output (1, 2). As the hypertension becomes established, long-term autoregulatory mechanisms act to restore cardiac output toward normal levels with the elevated blood pressure now being sustained by an elevated peripheral vascular resistance.

The mechanisms underlying this long-term autoregulatory control may differ from those mediating acute autoregulatory responses. Local autoregulatory responses to acute changes in blood flow can be rapidly achieved by transient alterations in vessel caliber. Long-term autoregulatory responses to a prolonged increase in cardiac output may, however, occur more slowly and involve structural modifications of the microvasculature. For example, a rarefaction of resistance vessels has been demonstrated among various vascular beds of the spontaneously hypertensive rat (SHR) (3–8) and other models of hypertension (9–12), including untreated hypertensive patients (13).

Because local autoregulatory mechanisms are active at the same level of the vascular tree as these reported structural changes (14), the possibility exists that such modifications of the microvasculature may alter the ability of a vascular bed to preserve normal acute autoregulatory function. Accordingly, experiments were conducted to determine whether the autoregulatory ability of skeletal muscle is affected during the developmental phase of spontaneous hypertension, and to assess further if these differences are correlated with an altered arteriolar responsiveness to changes in perfusion pressure. Local autoregulatory effectiveness was assessed in 6- and 9-week spontaneously hypertensive rats by comparing the change in blood flow for a given change in arterial pressure (gain), and by comparing the regression lines of pressure–flow curves constructed at these two ages.

A preparation utilizing the rat hindlimb was developed which permitted simultaneous

0037-9727/85 $1.50

measurements of hindlimb blood flow and pressure, as well as changes in diameter of resistance arterioles in the gracilis muscle. Because the majority of tissue that comprises the hindlimb is skeletal muscle, changes in the local control of blood flow in the gracilis muscle should be reflected in the total hindlimb blood flow.

Materials and Methods. Twenty-eight female spontaneously hypertensive rats and thirty Wistar–Kyoto (WKY) normotensive controls, 6 and 9 weeks old, were used in this study. The rats were bred in our own colony (NIH breeding stock) and maintained on a 12:12 light–dark cycle with access to food and water *ad libitum*.

Gracilis muscle preparation. A modification of the gracilis muscle preparation described by Henrich and Hecke (15) was developed for this study. The modifications permit *in vivo* microscopy of the *in situ* gracilis with its vasculature remaining intact.

Chloralose:urethane (2.5:10%) anesthesia was given ip (6 ml/kg) and supplemented as needed. A tracheostomy was performed to maintain a patent airway, and the right carotid artery catheterized to measure systemic arterial pressure. Body temperature was monitored rectally by a Telethermometer and maintained at 37°C by placing the rat on a circulating water heating mat.

The animal was placed on a restraining board with a height adjustable Lucite pedestal (18 mm od) and positioned so that the right leg extended around one side of the pedestal and the tail around the other. The superficial saphenous artery was catheterized (PE-90 with tip drawn to PE-10 size under heat) for blood pressure measurements at a point distal to the insertion of the gracilis muscle. A skin incision extending along the posterior medial border of the leg up to the pelvis was made and continued parallel to the abdominal wall. Care was taken to avoid cutting the branch of the superficial epigastric artery and vein which supplies the fat pad underlying the skin. The skin flap was reflected back and kept moist with a physiological saline solution (Normosol-R, pH 7.4; Abbott).

The gracilis was separated from the underlying semitendinosus and semimembranosus muscles, with the blunt dissection extending to the anterior border of the gracilis. The leg of the animal was firmly secured against the pedestal so that the gracilis rested atop the overlying coverslip. Three or four 5-O sutures in the connective tissue along the posterior border of the gracilis secured the muscle flat against the moistened coverslip. Tension was kept to a minimum. The connective tissue overlying the muscle was teased away and the tissue moistened and covered with Saran Wrap to reduce evaporation of tissue fluid. The surface temperature of the prepared leg was monitored using a thermistor probe and a Telethermometer. The surface temperature was maintained at 35–36°C with a 20-W high-intensity lamp and a temperature feedback system.

The muscle preparation was allowed to equilibrate 30 min prior to the start of the experiment. Preparations with visible hemorrhage from the muscle were not used. The presence of vasomotion, indicative of functioning local regulatory mechanisms, was also used to confirm the viability of the preparation. At the end of each experiment the right hindlimb was removed and weighed for normalizing femoral blood flow per 100 g of tissue.

Gracilis vasculature. The thinnest portion of the gracilis muscle lies in the anterior venter. This area ranges in thickness from about 75–100 μm in the youngest animals to over 300 μm in the 12-week animals. The arterioles visualized in this preparation were present in this area. The gracilis is supplied by a branch of the femoral artery. A main axial vessel (50+ μm) for each venter arises off this branch. These axial vessels divide into two longitudinal arterioles (30–40 μm) from which arise the 12- to 20-μm-diameter arterioles studied in these experiments.

In vivo microscopy. Changes in arteriolar internal diameter were measured via *in vivo* microscopy, using a Vickers microscope with Nikon water immersion or Zeiss dry objectives (10×) with a Zeiss 10× ocular. Images were projected through an RCA video camera (Model TC 1000) and recorded on magnetic video tape utilizing a Sony AV3600 video recorder for later analysis by video image shearing techniques (16). The final magnification of the vessel image on the monitor

screen was approximately 1300×. A fiber optic light source was used to reduce heating effects on the muscle. A green filter between the condenser and the preparation was used to enhance contrast between the red blood cells and the surrounding tissues.

Occluder design and placement. A noncannulating electromagnetic flow probe (Carolina Medical Electronics 100 series, 1.5-mm circumference) was placed around the right femoral artery. To control the downstream perfusion pressure an hydraulic occluder was also placed around the femoral artery distal to the flow probe. The occluder design was adopted from one originally described by Samar and Coleman (17). The cuff, made from Silastic (Dow Corning) tubing (0.132 in id × 0.183 in od) was 2–3 mm wide. A second Silastic tube (0.03 in id × 0.065 in od) was substituted for the latex balloon used by Samar and Coleman and was connected to a syringe by PE-50 tubing.

Filling the occluder balloon with a micrometer drive syringe produces a graded constriction. To damp the pressure which expands the balloon and thus permit a more precise control of the femoral occlusion, an air bubble was introduced into the tip of the syringe barrel.

The carotid and saphenous arterial pressures were measured by strain gauge transducers (Statham P23 and Ailtech MS-10C, respectively) and recorded. The pressure signal from the saphenous artery was also used as the X-axis input to an X–Y plotter. Output signals from the flowmeter were similarly fed into a recording oscillograph and the Y-axis of the plotter, thereby yielding on-line pressure–flow curves.

Pressure–flow studies. Pressure–flow relationships in the hindlimb were studied by occluding the femoral artery and then raising the hindlimb pressure in increments of 10–15 mm Hg until the original resting pressure was restored. Each pressure level was held until a stable flow was obtained. The resulting pressure–flow curve was plotted on-line for each animal. Because of hysteresis in the pressure–flow curves when the perfusion pressure was raised versus when the pressure was reduced, only ascending pressure–flow curves were used. In those cases where stable blood flow was not observed within 30 sec, or a pressure increase greater than 15 mm Hg resulted upon release of the occluder, a complete pressure–flow curve for that animal was not obtained.

The ability of the vascular bed to maintain a constant flow with changes in perfusion pressure is represented by the gain of the system. For each incremental change in perfusion pressure, the closed-loop gain of the autoregulatory control system was calculated, using the relationship (18, 19)

$$G = 1 - [(\Delta f/F)/(\Delta p/P)]$$

where F is the initial flow at a particular pressure range beginning at blood pressure P. The maximal change in flow and pressure over this particular range is represented by Δf and Δp, respectively. Thus $(\Delta f/F/\Delta p/P)$ is the slope of the pressure–flow curve at a given point with G representing the closed-loop gain of the system. A rigid, nonregulating system has a gain of 0, a perfectly regulating system a gain of 1. A negative value of G indicates that the change in flow is greater than the change in pressure, as might occur with passive distensible vessels. Positive values of G indicate that regulatory mechanisms have blunted the change in flow for the given pressure change. The point where the gain shifts from negative to positive represents the lowest perfusion pressure at which the vascular bed autoregulates.

A mean lower pressure limit for autoregulation (LPLAR) was calculated for each age and strain by averaging the individual lower limit pressures for a particular group. This LPLAR for individual animals was obtained by determining the pressure where the gain shifted from negative to positive. A mean gain for the autoregulatory range was calculated by averaging the net gain over the regulatory range for each of the animals. Using the mean LPLAR to divide the pressure–flow curve into a discrete upper autoregulatory range and a lower passive range, regression lines were calculated for the two portions of the curve and the slopes of the two lines compared.

Statistical analyses. All data are presented as means ± standard error of the mean. Statistical significance was determined by analysis of variance for repeated measures, and by t test for unpaired variables.

Results. The basic characteristics of the animals used in this study are presented in Table I. Body weights of both strains were similar at 6 and 9 weeks of age, as were the right hindlimb weights. The ratio of hindlimb weight to body weight ranged from 0.072 to 0.077.

Mean arterial blood pressure was significantly elevated in both the carotid and saphenous arteries of the SHR at both ages ($P < 0.001$). Heart rates, determined from the carotid artery pressure tracing, were also elevated ($P < 0.001$) in the SHR. Resting femoral artery blood flow was 22% higher ($P < 0.01$) in the SHR compared to that of the WKY at 6 weeks. At 9 weeks, however, femoral blood flow in the SHR was comparable to that measured in the WKYs. Hindlimb vascular resistance in the SHR was 26% higher ($P < 0.01$) than that in the WKY at 6 weeks of age, and 77% higher at 9 weeks ($P < 0.01$). These data illustrate that from 6 to 9 weeks of age peripheral vascular resistance assumed a greater role in the progressive increase in blood pressure. By 9 weeks of age the influence of the increased flow in supporting the elevated blood pressure was clearly diminished. Vascular resistance calculated at the LPLAR was also greater in the SHR at 6 and 9 weeks.

The composite pressure–flow curves for the 6 and 9 week WKYs and SHRs are presented in Figs. 1 and 2. For both strains the mean saphenous arterial pressure occurred within the pressure range over which that particular group was able to regulate flow. By analysis of variance the pressure–flow curves of the SHR were shifted to the right at both ages ($P < 0.05$). The greater disparity between the two curves at 9 weeks reflects a rightward shift by the SHR, a change consistent with the increasing vascular resistance (Table I).

The LPLAR in the SHR exhibited an upward shift ($P < 0.02$) at 6 and 9 weeks (Table II; Figs. 1 and 2). This upward resetting (58 and 80%, respectively, relative to the LPLAR of the WKY) was reflected directly by comparable increases in the SHR saphenous artery blood pressure. In the WKY, whose carotid and saphenous artery pressures did not vary between 6 and 9 weeks, the LPLAR did not shift. Femoral blood flow at the LPLAR of the 6-week SHR, like that measured at the resting blood pressure, was elevated ($P < 0.01$) when compared to the WKY. At 9 weeks, however, this femoral blood flow was equivalent in the two strains (Table I).

The closed-loop gains describing the autoregulatory capacity over the pressure–flow curves are presented in Table II. Across the autoregulatory pressure range the gain of the system did not vary statistically with age for either the WKY or the SHR. Between strains, the gains for the SHR at both ages tended to

TABLE I. BODY WEIGHT AND HEMODYNAMIC PARAMETERS OF 6- AND 9-WEEK OLD WKYs AND SHRs

	6 Week		9 Week	
	WKY	SHR	WKY	SHR
Body weight[a] (g)	103 ± 3	106 ± 2	148 ± 5	154 ± 3
Carotid MAP (mm Hg)	92 ± 3	134 ± 4***	89 ± 4	162 ± 4***
Saphenous MAP (mm Hg)	82 ± 3	124 ± 3***	76 ± 4	141 ± 4***
Heart rate (bpm)	381 ± 16	466 ± 11***	355 ± 11	413 ± 10***
Femoral flow	9.2 ± 0.5	11.2 ± 0.5**	8.8 ± 0.4	9.3 ± 0.5
LPLAR[b] femoral flow	5.12 ± 0.49	7.36 ± 0.42**	6.03 ± 0.48	6.32 ± 0.43
Hindlimb resistance	9.1 ± 0.5	11.5 ± 0.6***	8.8 ± 0.4	15.6 ± 0.7***
LPLAR resistance	8.3 ± 0.8	10.5 ± 0.7*	8.6 ± 0.6	13.6 ± 0.8***
N	15	15	15	13

[a] Data are means ± SEM; resistance units: mm Hg · min/ml · 100 g; Flow: ml/min/100 g.
[b] LPLAR = lower pressure limit of autoregulation.
* $p < 0.05$ vs WKY.
** $p < 0.01$ vs WKY.
*** $p < 0.001$ vs WKY.

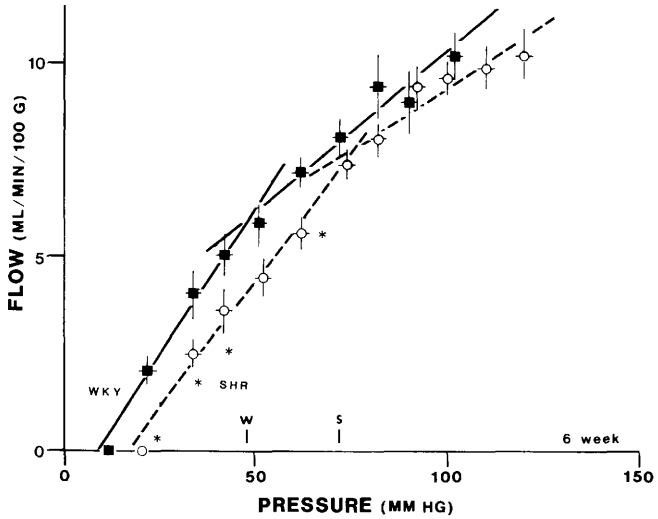

FIG. 1. Hindlimb pressure–flow curves of 6-week-old WKY and SHR rats. Data points (mean ± SEM) are connected by regression lines above and below the LPLAR, indicated by a W and S for WKY and SHR, respectively. *$P < 0.05$ vs WKY at same pressure.

be lower, but these differences were not statistically significant. Below the LPLAR, passive control of hindlimb blood flow (a negative gain value) was similar between the WKYs and SHRs at each age, and were statistically similar with age within strain.

Autoregulatory control, reflected by the slope of the regression lines above and below the LPLAR, was also compared in the two strains (Table III). For both hypertensive and normotensive animals, the slope describing the autoregulatory range was significantly less than that describing the passive, nonregulatory range. Between strains, the slopes of the

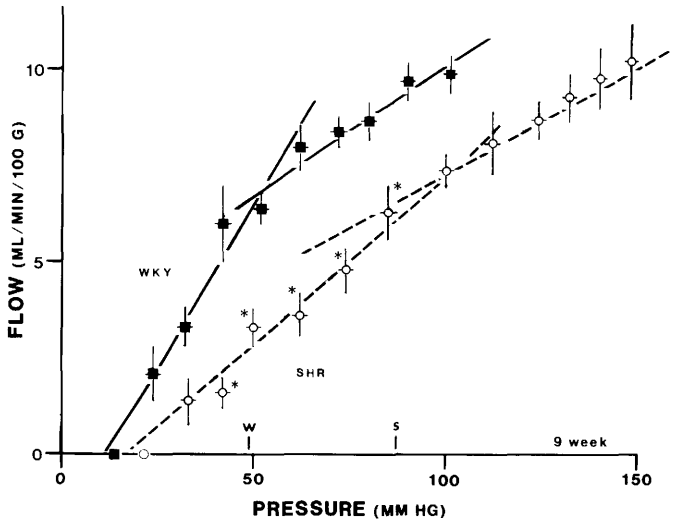

FIG. 2. Hindlimb pressure–flow curves of 9-week-old WKY and SHR rats. Data points (mean ± SEM) are connected by regression lines above and below the LPLAR, indicated by a W and S for WKY and SHR, respectively. *$P < 0.05$ vs WKY at same pressure.

TABLE II. LOWER PRESSURE LIMIT OF AUTOREGULATION (LPLAR) AND MEAN GAIN VALUES DURING DEVELOPMENT OF HYPERTENSION IN THE SHR

	LPLAR		Mean gain autoreg range		Mean gain passive range	
Weeks	WKY	SHR	WKY	SHR	WKY	SHR
6	46.2 ± 4.4[a] (15)	72.8 ± 3.7** (15)	0.40 ± 0.06 (15)	0.32 ± 0.05 (15)	−1.74 ± 0.50 (15)	−1.62 ± 0.60 (15)
9	49.2 ± 3.0 (15)	88.8 ± 5.0** (13)	0.46 ± 0.07 (15)	0.30 ± 0.07 (13)	−2.82 ± 0.64 (15)	−1.93 ± 0.57 (13)

[a] Data are means ± SEM; sample size in parentheses.
** $p < 0.0001$ vs WKY.

autoregulatory section of the pressure–flow curves were statistically similar at both 6 and 9 weeks. Below the LPLAR, however, the slope of the regression line was markedly damped ($P < 0.01$) in the 9-week SHR.

The changes in arteriolar diameter with changes in hindlimb perfusion pressure are presented in Figs. 3 and 4. At pressures below the LPLAR the arteriolar diameters are at or near their maximum observed diameters. Arterioles of the SHR at 9 weeks exhibit a greater diameter than those of the WKY. When compared at pressures just below their respective resting arterial pressures, no difference in arteriolar diameter was apparent between the hypertensive and normotensive animals. As hindlimb blood pressure was increased, a vasoconstriction of the gracilis muscle arterioles occurred. The onset of this autoregulatory response closely coincided with the respective LPLAR for the WKYs and SHRs at each age.

TABLE III. SLOPES OF REGRESSION LINES ABOVE AND BELOW THE LOWER PRESSURE LIMIT OF AUTOREGULATION

	Slope of regression line			
	Below limit pressure		Above limit pressure	
Age	WKY	SHR	WKY	SHR
6 Weeks	0.175	0.133	0.085[a]	0.061[a]
9 Weeks	0.175	0.087**	0.066[a]	0.059[b]

[a] Slope above and below limit is different within strain, $P < 0.01$.
[b] Slope above and below limit is different within strain, $P < 0.03$.
** $P < 0.01$ vs WKY.

Discussion. Pressure–flow curves were generated during the developmental phase of hypertension to determine whether the acute autoregulatory mechanism of skeletal muscle was altered in the SHR. Simultaneous measurements of arteriolar diameters in the gracilis muscle were made to assess possible differences in microvascular reactivity during the acute autoregulatory responses. Two major differences immediately distinguished the pressure–flow curves of the hypertensive animals from the controls. The increasing hindlimb resistance observed in the SHR at 6 and 9 weeks (Table I) was reflected in the rightward shifts of the SHR pressure–flow curves at each of these ages (Figs. 1 and 2). Second, at both ages the LPLAR of the SHR exhibited a significant upward shift (Table II) relative to that of the WKY.

An upward shift of the LPLAR has also been reported for the cerebral circulation of the SHR (20) and for the cerebral circulation of baboons with established Goldblatt renovascular hypertension (21). These upward resettings of the LPLAR may reflect an upward shift of the entire autoregulatory range. Strandgaard *et al.* (22) observed an upward shift in the upper limit of autoregulation in baboons with Goldblatt hypertension. Similarly, Overbeck and co-workers (23) reported an upward shift in their studies on pump perfused forelimbs of dogs with one-kidney Goldblatt hypertension.

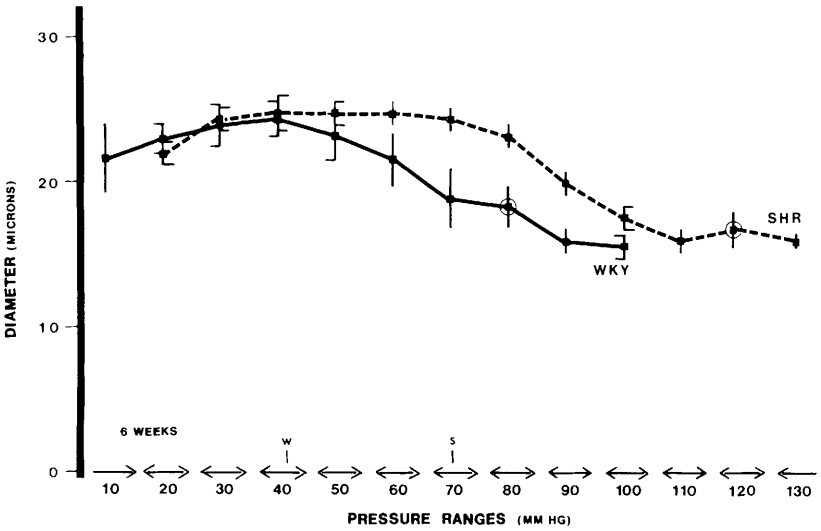

FIG. 3. Changes in gracilis muscle arteriolar diameter with changes in hindlimb perfusion pressure for 6-week-old WKY and SHR rats. Diameter at resting arterial pressure is circled. W and S indicate the LPLAR for WKY and SHR, respectively. Data are means ± SEM.

The experimental protocol of the present study did not allow us to discern whether the upward shift of the LPLAR in the SHR was a causal factor in the hypertension or whether it was a response to the elevated blood pressure. It was noted, however, that at both 6 and 9 weeks the LPLAR was 56–59 and 63–65%, respectively, of the saphenous MAP for both the WKY and SHR. Such similarity in the relative position of the LPLAR is consistent with the idea that the LPLAR set point is a response to the hypertension and not a mitigating cause.

A positive pressure intercept of the pressure–flow plot, often observed in pressure–flow studies (24), was observed for both the WKY and SHR (Figs. 1 and 2). While the basis for this is not clear, it has been explained in terms of a rapid vessel closure when the decreasing blood pressure reached a critical closing pressure. In the present study, this intercept pressure was higher in the SHR at both 6 and 9 weeks. A possible explanation for this difference is a decreased drainage of the SHR vasculature resulting from the reduced vessel density of these hypertensive animals (3, 6, 25).

The pressure–flow curves of the two strains also exhibited some important similarities. Changes in arteriolar diameter are the most efficient means of altering resistance and thereby regulating flow. This gracilis muscle preparation allowed for analysis of microvascular changes occurring as the perfusion pressure was varied. In both the WKY and SHR the pressure at which vasoconstriction of the gracilis muscle arterioles was first observed was closely associated with the LPLAR, the onset of the autoregulatory response (Figs. 3 and 4). This arteriolar response was evident at both 6 and 9 weeks. At pressures below the LPLAR, the arterioles were dilated, with the diameters remaining nearly constant.

The similarity of these vasoconstrictor responses attains greater significance when viewed in conjunction with the calculated closed-loop gains and the slopes of the autoregulatory portion of the pressure–flow curves. No differences in these two parameters which describe the autoregulatory capacity of the hindlimb were detected between the hypertensive and normotensive rats at either age (Tables II and III). The absence of a difference among these three variables between the two groups clearly suggests that the acute autoregulatory mechanism of the SHR was not adversely affected by the developing hypertension at either age.

However, the rightward shift of the SHR pressure–flow curves, evidence for an in-

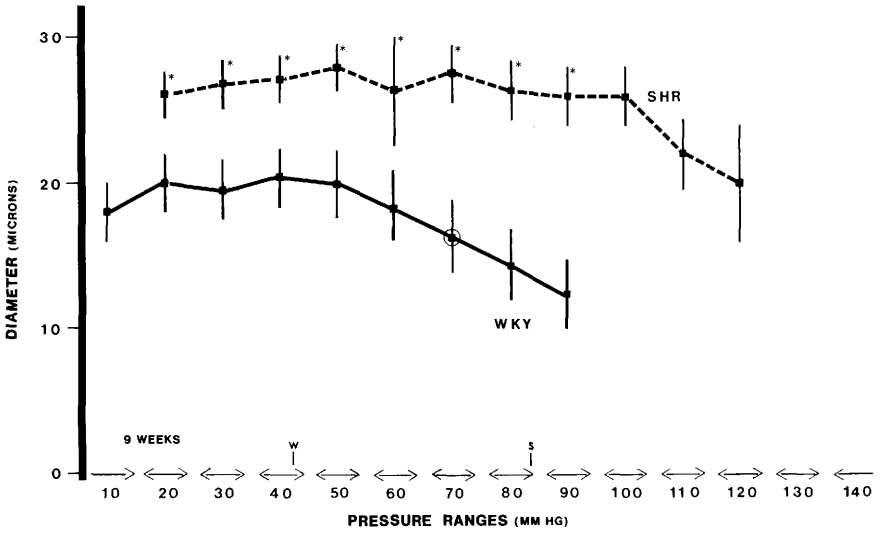

FIG. 4. Changes in gracilis muscle arteriolar diameter with changes in hindlimb perfusion pressure for 9-week-old WKY and SHR rats. Diameter at resting arterial pressure is circled. W and S indicate the LPLAR for WKY and SHR, respectively. Data are means ± SEM.

creasing vascular resistance, does support the occurrence of a structurally based long-term autoregulatory mechanism responsive to overperfusion of the tissues. At the beginning of the 3-week experimental period, resting hindlimb blood flow, as well as flow at the LPLAR was elevated in the SHR. Three weeks later these measures of hindlimb blood flow had returned to control levels with the continued rise in blood pressure being sustained by vascular resistance which continued to rise (Table I).

These concurrent changes in systemic blood pressure, blood flow, and resistance during the development of the hypertension are consistent with the concept of a long-term total body autoregulation (2, 26) for restoring cardiac output to normal. In a previous study, Smith and Hutchins (2) observed that the cardiac index of conscious, unrestrained SHRs, was also elevated at 6 weeks of age, and was supporting the elevated blood pressure. But at 12 weeks of age, even though blood pressure was still elevated, the cardiac index was not different from that of the normotensive WKYs. The result of these hemodynamic changes was that the blood pressure elevated initially by a greater than normal cardiac output was eventually sustained by a rising vascular resistance as cardiac output returned to normal. This greater resistance is evidenced in the rightward shift of the pressure–flow curve among the hypertensive rats (Figs. 1 and 2).

This apparent dissociation between mechanisms affecting long-term autoregulatory responses to increased cardiac output and tissue perfusion, and short-term responses to local changes in perfusion may be founded in specific structural alterations in the microvasculature. It is well understood that several factors can alter the resistance of a vascular bed, the most significant being arteriolar diameter and arteriolar number. Interestingly, the long-term autoregulatory mechanism does not appear to be invoking vasoconstriction as a regulatory response. Arteriolar diameters at both the resting blood pressure and the LPLAR are equivalent or even slightly dilated in the SHR (Figs. 3 and 4). Prior experiments in our laboratory (3, 4, 25) and in others (5, 27, 28) have likewise failed to demonstrate sufficient vasoconstriction among the small resistance vessels of skeletal muscle in the SHR to account consistently for the characteristic long-term increase in vascular resistance.

Medial hypertrophy of arterioles has been proposed as the structural basis for this increased resistance in the SHR (29). However,

in the SHR this increase in wall:lumen ratio has been observed only among mesenteric arterioles greater than 150 μm in diameter (30). With renovascular hypertension a medial thickening may occur among smaller arterioles (12, 31).

More distal in the microcirculation, vascular rarefaction has been demonstrated in both animal and clinical studies of hypertension. Short (32) using an arteriographic technique, observed a diminished vessel density in the intestinal submucosa of patients with established hypertension. More recently, Hutchins and Darnell (3) reported a significant rarefaction among the smaller resistance vessels in the cremaster muscle of the SHR. They proposed that such a vascular deficit among the resistance vessels was a pivotal underlying mechanism governing the long-term autoregulatory response to an elevated blood pressure. This arteriolar rarefaction in the cremaster has since been confirmed (4, 5, 25) and extended to other vascular beds in the SHR (6–8) as well as to other models of hypertension (9–13). A reduction in the number of parallel vessels provides an effective means for maintaining a chronically elevated peripheral vascular resistance while maintaining diameters consistent with their functional position in the vascular tree. That is, the absence of a consistent and definitive vasoconstriction assures that these vessels can exert bidirectional control (vasodilatation and vasoconstriction) in regulating local blood flow. The activity of the local autoregulatory response is merely reset to operate at a higher pressure level in a manner analogous to the resetting of the baroreceptors in hypertension (33).

A difference in the acute pressure–flow characteristics between the WKY and SHR animals is indicated at pressures below the LPLAR, the passive range of flow control (Table II). A damping of the slope over this range as well as a higher calculated gain is evident for the SHR at 9 weeks, although this latter is not statistically significant ($P < 0.30$). A decreased vascular compliance of the SHR vessels and/or an increased wall:lumen ratio among arterioles larger than 100 μm in diameter may account for this. As vascular resistance is primarily regulated at this more distal level of the vascular tree, the changes in the larger arterioles are most likely a structural response to the increased pressure seen by these vessels.

This study was supported by HL-5392, HL-13936, and the North Carolina Heart Association. This investigation comprised part of the doctoral dissertation for Dr. Alson, the entire portion of which is available from University Microfilms, Ann Arbor, Mich.

1. Lund-Johansen P. Hemodynamic alterations in hypertension—Spontaneous changes and effects of drug therapy. A review. Acta Med Scand (Suppl)**603**:1–14, 1977.
2. Smith TL, Hutchins PM. Central hemodynamics in the developmental stage of spontaneous hypertension in the unanesthetized rat. Hypertension **1**(5):508–517, 1979.
3. Hutchins PM, Darnell AE. Observation of a decreased number of small arterioles in spontaneously hypertensive rats. Circ Res (Suppl I)**34/35**:161–165, 1974.
4. Dusseau JW, Hutchins PM. Stimulation of arteriolar number by salbutamol in spontaneously hypertensive rats. Amer J Physiol **236**:H134–H140, 1979.
5. Chen IIH, Prewitt RL, Dowell RF. Microvascular rarefaction in spontaneously hypertensive rat cremaster muscle. Amer J Physiol **241**:H306–H310, 1981.
6. Prewitt RL, Chen IIH, Dowell RF. Development of microvascular rarefaction in the spontaneously hypertensive rat. Amer J Physiol **243**:H243–H251, 1982.
7. Henrich H, Hertel R, Assman R. Structural differences in the mesentery microcirculation between normotensive and spontaneously hypertensive rats. Pflugers Arch **375**:153–159, 1978.
8. Haack DW, Schaffer JJ, Simpson JG. Comparisons of cutaneous microvessels from spontaneously hypertensive, normotensive Wistar-Kyoto and normal Wistar rats. Proc Soc Exp Bio Med **164**:453–458, 1980.
9. Sokolova IA, Rodionov IM, Blinkov SM. Rarefaction of capillary network in the brain of rats with induced DOCA-saline and renal hypertension. Microvasc Res **22**:125–126, 1981.
10. Webb DR, Jokelainen PT. Cerebral vascular rarefaction in DOCA/NaCl hypertensive rats. Anat Rec **196**:200a, 1980. [Abstract]
11. Prewitt RL, Rapp JP. Rarefaction of arterioles in Dahl-S hypertensive rat gracilis muscle. Microvasc Res **27**:259, 1984. [Abstract]
12. Prewitt RL, Chen IIH, Dowell RF. Microvascular alterations in the 1-kidney, 1-clip renal hypertensive rat. Amer J Physiol **246**(5):H728–H733, 1984.
13. Harper RN, Moore MA, Marr MC, Watts LE, Hutchins PM. Arteriolar rarefaction in the conjunctiva of human essential hypertensives. Microvasc Res **16**:369–372, 1978.

14. Morff RJ, Granger HJ. Autoregulation of blood flow within individual arterioles in the rat cremaster muscle. Circ Res **51**:43–55, 1982.
15. Henrich HN, Hecke A. A gracilis muscle preparation for quantitative microcirculatory studies in the rat. Microvasc Res **15**:349–356, 1978.
16. Intaglietta M, Tompkins WR. Microvascular measurements by video image shearing and splitting. Microvasc Res **5**:309–312, 1973.
17. Samar RE, Coleman TG. Mean circulatory pressure and vascular compliances in the spontaneously hypertensive rat. Amer J Physiol **237**(5):H584–H589, 1979.
18. Norris CP, Barnes GE, Smith EE, Granger HJ. Autoregulation of superior mesenteric flow in fasted and fed dogs. Amer J Physiol **237**:H174–H177, 1979.
19. Shepherd AP. Intestinal blood flow autoregulation during foodstuff absorption. Amer J Physiol **239**: H156–H162, 1980.
20. Fujishima M, Omae T. The lower limit of cerebral autoregulation in normotensive and spontaneously hypertensive rats. Experientia **32**:1019–1020, 1976.
21. Jones JV, Fitch W, MacKenzie ET, Strandgaard S, Harper AM. Lower limit of cerebral blood flow autoregulation in experimental renovascular hypertension in the baboon. Circ Res **39**:555–557, 1976.
22. Strandgaard S, Jones JV, MacKenzie ET, Harper AM. Upper limit of cerebral blood flow autoregulation in experimental renovascular hypertension in the baboon. Circ Res **37**:164–167, 1975.
23. Overbeck HW, Swindall BT, Cowan DF, Fleck MC. Experimental renal hypertension in dogs: Forelimb hemodynamics. Circ Res **29**:51–62, 1971.
24. Alexander RS. Critical closure reexamined. Circ Res **40**(6):531–535, 1977.
25. Hutchins PM, Dusseau JW, Marr MC, Greene AW. The role of arteriolar structural changes in hypertension. In: Henrich H, ed. Microvascular Aspects of Spontaneous Hypertension. Bern, Hans Huber, pp41–53, 1982.
26. Coleman TG, Granger HJ, Guyton AC. Whole body circulatory autoregulation and hypertension. Circ Res (Suppl II)**28/29**:76–87, 1971.
27. Bohlen HG, Gore RW, Hutchins PM. Comparison of microvascular pressures in normal and spontaneously hypertensive rats. Microvasc Res **13**:125–130, 1977.
28. Bohlen HG, Lobach D. In vivo study of microvascular wall characteristics and resting control in young and mature spontaneously hypertensive rats. Blood Vessels **15**:322–330, 1978.
29. Folkow B, Hallback M, Lundgren Y, Sivertsson R, Weiss L. Importance of adaptive changes in vascular design for establishment of primary hypertension studied in man and in spontaneously hypertensive rats. Circ Res **32**(Suppl I):2–16, 1973.
30. Mulvany MJ, Hansen PK, Aalkjaer C. Direct evidence that the greater contractility of resistance vessels in spontaneously hypertensive rats is associated with a narrowed lumen, a thickened media, and an increased number of smooth muscle cell layers. Circ Res **43**:854–864, 1978.
31. Furuyama M. Histometrical investigation of arteries in reference to arterial hypertension. Tohoku J Exp Med **76**:388–414, 1962.
32. Short DS. Arteries of intestinal wall in systemic hypertension. Lancet **2**:1261–1263, 1958.
33. Sapru HH, Wang SC. Modification of aortic baroreceptor resetting in the spontaneously hypertensive rat. Amer J Physiol **230**:664–674, 1976.

Received February 8, 1985, P.S.E.B.M. 1985, Vol. 180.
Accepted April 12, 1985.